

Numerical simulation of dust explosion in the spherical 20l vessel

Z. SALAMONOWICZ^{1*}, M. KOTOWSKI², M. PÓŁKA¹, and W. BARNAT²

¹ Faculty of Fire Safety Engineering, Main School of Fire Service, 52/54 Słowackiego St., 01-629 Warsaw, Poland

² Faculty of Mechanical Engineering, Department of Mechanics and Applied Computer Science, Military University of Technology, 2 Kaliskiego St., 00-908 Warsaw, Poland

Abstract. The paper presents experimental and numerical validation of the combustion process of coal and flour dust dispersed in a spherical chamber of 20 cubic decimetres volume. The aim of the study is to validate the numerical simulation results in relation to the experimental data obtained on the test stand. To perform the numerical simulations, a Computational Fluid Dynamics code FLUENT was used. Geometry of the computational domain was built in compliance with EN 14460. Numerical simulations were divided into two main steps. The first one consists in a dust dispersion process, where influence of standardized geometry was verified. The second part of numerical simulations investigated dust explosion characteristics in compliance with EN 14034. After several model modifications, outcomes of the numerical analysis shows positive agreement with both, the explosion characteristics for different dust concentration levels and the maximum pressure increase obtained on the test stand.

Key words: dust explosion, CFD, spherical 20l vessel.

1. Introduction

The dust particles with different size distribution are created during many technological processes where friction, cutting etc. occur. If processed material has flammable properties, resultant dust will create explosion threat [1]. In case of formation of dust and air mixture in technological processes, the threat is much bigger. Dusty atmosphere creates a particularly high risk in coal mines and cereal mills [2]. One of the methods used to reduce effects of the air and dust mixtures' explosion is use of a relief surfaces or a relief valve [3, 4]. The main task of the relief valve is to open protected area to atmosphere after achieving given level of overpressure. Such controlled release of explosion's energy to environment reduces the risk of the apparatus damage and the potential damage to infrastructure. However, sometimes there is no possibility to release apparatus contents to the atmosphere. The solution for the above situation is to design the equipment with strength capabilities exceeding foreseen overpressure generated during the explosion.

Determination of the pressure value, created during the explosion of a particular dust-air mixture, is most often achieved through the test explosions of dust in standardized tanks [5–8]. A very popular method which gains more and more acknowledgment is the use of numeral CFD techniques [9, 10] for simulation of dust and air mixtures' explosions in areas of the processing equipment. FLACS (FLame ACceleration Simulator) model developed by Hjertager and others [11], was used as a calculation engine in creation of DESC (Dust Explosion Simulation Code). Skjold and others [12] based DESC on standard explosiveness indicator K_{st} . Other approaches were chosen by German scientists Krause and Kasch [13], who used popular CFD program FLUENT and a chemical

reaction model based on the devolatilised solid particles and burning created gas phase. Krause and Kasch used the Arrhenius combustion reaction model for laminar combustion and the Magnussen-Hertjager model for turbulent combustion.

2. Experiments

Two dusts were used for the research: the hard coal acquired from the Barbara coal mine and the wheat *Szymanowska* flour, type 480. In accordance with the standards, both dusts were sifted through the sieve with square holes with nominal size of 200 μm . The dust with a size distribution within the mentioned range was used to determine explosiveness parameters. Coal contents: 91% of clean coal, 6.9% of volatile components, 2.1% of ash. Contents of the flour and physical and chemical properties were assumed in accordance with PN-B-02852 standard for the 480 type [14]. The following material parameters were used for the numerical analysis [15, 16] (specified in chart 1 below): ρ – density, λ – thermal conductivity coefficient, Q – heat of combustion and c – specific heat.

2.1. Coal and flour dust explosions. Determination of the dusts' explosiveness parameters was carried out on the research station which abides the EN 14034 *Determination of explosiveness characteristics of dust clouds* standard [6]. The station was equipped with a spherical tank, quick pneumatic valve, dust tank, dispersion nozzle inside the spherical tank, steering valves and coat cooling installation.

Determined parameters for the chosen dusts for the purposes of this article are as follows: the maximum pressure of explosion (p_{max}) and the maximum rate of pressure rise $(dp/dt)_{\text{max}}$. The maximum pressure of explosion is a max-

*e-mail: zsalamonowicz@sgsp.edu.pl

imum value of overpressure during explosion of explosive atmosphere in the range of combustible concentration of dust in a closed tank. The maximum rate of a pressure rise is a maximum value of pressure increase within a time unit during explosion of explosive atmosphere in the range of combustible concentration of dust in a closed tank.

Table 1
Material parameters of studied dusts

Dust	ρ [g/cm ³]	λ [W/m/K]	Q [MJ/kg]	c [J/kg/K]
Coal	1.55	0.045	32.79	1680
Flour	1.51	0.100	15.00	1423

The test tank is an explosion-proof sphere (up to EN 14034 standard) made of stainless steel, with the capacity of 20 dm³ (1). The tank has water coat for abstraction of explosion heat and pressurized container for dust (2), from which, through a quick discharge valve (3) and a dispersion nozzle, dusts disperse into the tank. A quick discharge valve is pneumatically opened and its valves are electrically operated. The ignition source is placed close to the centre of the tank. In addition, the tank is equipped in the pressure and oxygen concentration measurement system.

The initial conditions of experiment were determined in accordance with the standard: pressure in a dust container with loaded dust – 20 bar, pressure in the spherical tank – lowered to 0.4 bar, temperature – 20°C, ignition delay – 60 ms, ignition source – 2 pyrotechnical fuses, 5 kJ each placed close to the sphere centre. After opening of the pneumatic discharge valve, the dust is transferred to the spherical chamber, then valve closes and delayed ignition of a dust cloud occurs. To determine searched parameters pressure within time function is measured.



Fig. 1. Test apparatus to determination of explosion characteristics dust clouds: 1 – 20 dm³ explosion-proof sphere, 2 – dust container, 3 – fast discharge valve

2.2. Numerical simulations. The numerical research was conducted in the FLUENT environment which belongs to the CFD (Computational Fluid Dynamics) programs' group [17]. The CFD programs allow to find necessary information about

a fluid flow (layout of speed field, pressure field), heat transfer (temperature field) and mass (including chemical reactions). It is achieved through the numerical solution of equations describing exchange of momentum, energy and mass balance.

Each flow occurrence modelled in Fluent is solved on the basis of the continuity equation, the energy equation and mass balance. Another approach to the application of energy balance equations are presented in the work [18, 19]. The continuity Eq. (1) in its general form is important for compressible as well as non-compressible flows

$$\frac{\partial p}{\partial t} + \nabla \cdot (p\bar{v}) = S_m, \quad (1)$$

where p – static pressure, t – time, v – speed, S_m – added mass to continuous phase e.g. as a result of vaporization of particles in multiphase flows. For two-dimensional symmetrical axis issue, this equation is described with following formula (2)

$$\frac{\partial p}{\partial t} + \frac{\partial}{\partial x}(pv_x) + \frac{\partial}{\partial r}(pv_r) + \frac{pv_r}{r} = S_m, \quad (2)$$

where x – axis coordinate, r – radial coordinate, v_x – axis speed, v_r – radial speed. Equation of momentum conservation is described with the following formula (3)

$$\frac{\partial p}{\partial t}(p\bar{v}) + \nabla \cdot (p\bar{v}\bar{v}) = -\nabla p + \nabla \cdot (\tau) + p\bar{g} + \bar{F}, \quad (3)$$

where τ – stress tensor, $p\bar{g}$ – gravity forces, \bar{F} – external forces. Stress tensor is a tensor described with the following formula (4)

$$\tau = \mu[(\nabla\bar{v} + \nabla\bar{v}^T) - \frac{2}{3}\nabla \cdot \bar{v}I], \quad (4)$$

where μ – dynamic viscosity, I – individual tensor. During dust dispersion from the dust tank to the sphere's interior, aerodynamic field F of decompressed gas affects particles which are in the flow field. Force is calculated with following formula (5)

$$F = \frac{\pi d^2}{4} C_d \frac{\rho_1(u_1 - u_2)u_1 - u_2}{2}, \quad (5)$$

where ρ_1 – gas density, C_d – aerodynamic drag coefficient, d – diameter of dust particles, u_1 – gas flow speed, u_2 – speed of dust particle. It was assumed in this study, that the accelerated particles are ideal spheres for which aerodynamic drag used in FLUENT program is described with following formula (6) defined by Morsi and Alexander model

$$C_d = A_1 + \frac{A_2}{Re} + \frac{A_3}{Re^2}, \quad (6)$$

where the relative Reynolds number which characterize flow is described with following dependency (7)

$$Re = \frac{\rho_1 d |u_1 - u_2|}{\mu}, \quad (7)$$

where Re – Reynolds number for the particle, μ – dynamic fluid viscosity. Numerical model finds solutions of the problem taking into account formulas of energy and mass as well as

standard k - ε turbulence model [20] described with following formulas (8) and (9):

$$\frac{\partial}{\partial t}(\rho k) + \frac{\partial}{\partial x_i}(\rho k v_i) = \frac{\partial}{\partial x_j} \left[\left(\mu + \frac{\mu_t}{\sigma_k} \right) \frac{\partial k}{\partial x_j} \right] + G_k + G_b + \rho \varepsilon - Y_M, \quad (8)$$

$$\frac{\partial}{\partial t}(\rho \varepsilon) + \frac{\partial}{\partial x_i}(\rho \varepsilon v_i) = \frac{\partial}{\partial x_j} \left[\left(\mu + \frac{\mu_t}{\sigma_\varepsilon} \right) \frac{\partial \varepsilon}{\partial x_j} \right] + C_{1\varepsilon} \frac{\varepsilon}{k} (G_k + C_{3\varepsilon} G_b) - C_{2\varepsilon} \rho \frac{\varepsilon^2}{k}, \quad (9)$$

where k – turbulent kinetic energy, ε – energy dissipation coefficient, G_k – represents generation of turbulent kinetic energy through average speed gradient, G_b – through lift forces, Y_M – influence of dilatation fluctuation, $C_{1\varepsilon}$ – $C_{3\varepsilon}$ – constants, σ_k and σ_ε – Prandtl turbulent numbers for k and ε .

The Eulerian type model was used for modelling. It allows modelling of divided and mutually interacting phases. It may be gas, solid or liquid phases in almost every configuration. Each phase is treated as continuous, no matter if it is the gas phase, liquid in the form of fluid or only few drops or solid in a form of powder or dust as in this case. The interaction between e.g. a solid phase in a form of dust and gas phase depends on a size of solid phase particles, but in behaviour equations this phase is modelled as continuous, so instead of parameters of single particles of a phase, average values of phase particles. Such an approach allows to significantly decrease costs of numerical calculation and modelling of big scale multiphase flows. Size of calculation mesh cannot be too small. It must be at least one order of magnitude bigger than a size of particles in a solid phase. In case of too small cells in comparison with a size of particles, the model becomes non-physical and a solid particles phase cannot be treated as continuous. The volumetric model was used for modelling of occurring chemical reactions. It used Arrhenius equations which uses heat oscillation frequency, temperature and process activation energy for each of researched materials. The values of particular used coefficients are close to the values which are generally accessible in the dedicated literature.

3. Results and discussion

3.1. Explosion characteristics. Result of experiments carried out for coal and flour dusts are presented in diagrams 2 and 3. Diagrams show changes of pressure (p_{ex}) in research tank during particular experiments. Change of pressure proceeds from 0.4 bar to normal pressure 1.013 bar after opening of the valve and movement of the dust to spherical chamber. In the next step discharge valve is closed and after 60 ms delay the ignition of dust cloud occurs through 2 pyrotechnical fuses 5 kJ each. In the further part of the diagram we observe deflagration burning the of dust cloud. Due to the cooling effects and pressure effects caused by chemical igniters, a standard includes correction according to the following Eqs. (10)–(12):

$$p_{\max} = 0.775 p_{ex}^{1.15} \quad \text{for } p_{ex} \geq 5.5 \text{ bar}, \quad (10)$$

$$p_{\max} = \frac{5.5 (p_{ex} - p_{ci})}{5.5 - p_{ci}} \quad \text{for } p_{ex} < 5.5 \text{ bar}, \quad (11)$$

$$p_{ci} = \frac{1.6 E_i}{10000}, \quad (12)$$

where p_{\max} – maximum pressure of explosion after correction in bar, p_{ex} – experimental pressure in bar, E_i – igniters energy in J.

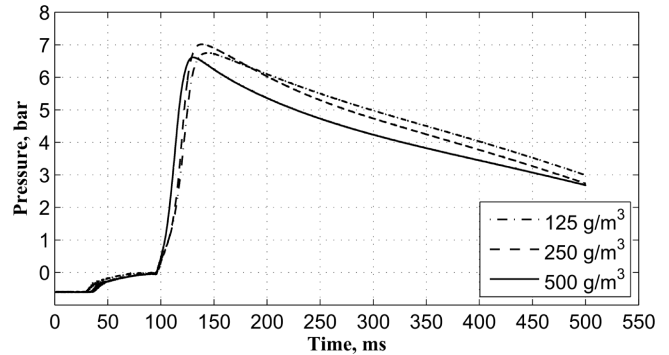


Fig. 2. Pressure changes during explosion for coal

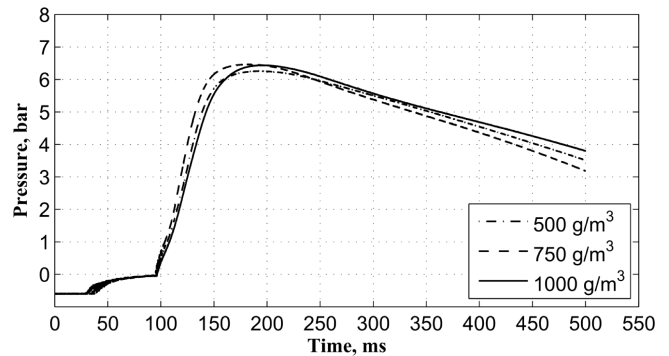


Fig. 3. Pressure changes during explosion for flour

3.2. Numerical simulations characteristics. The numerical model was simplified through the elimination of a bend in the dust supply system and setting the tank in the axis of sphere symmetry simultaneously with retention of the intake system length between dust tank and dispersion nozzle in the sphere. It helped to minimize analysed model to a two-dimensional symmetrical to axis problem. Simultaneously we omitted the thickness of materials used for a test stand building, building the model on the basis of data necessary to project the geometry directly interacting with the flow. Figure 4 presents numerical model geometry.

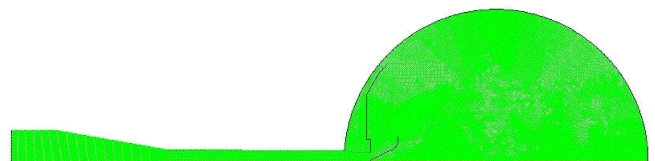


Fig. 4. Geometry of numerical model

The numerical simulations, as well as the experiment, consisted of two stages: discharge of the dust and combustion and

deflagration processes. The process of coal dust discharging is shown in Fig. 5. It illustrates chosen 3 moments of dust movement (speed of particles in time 4, 10 and 40 ms).

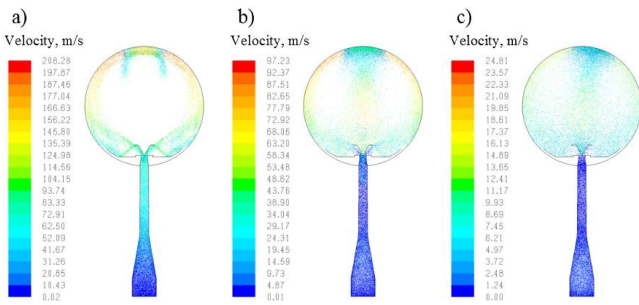


Fig. 5. Phase of coal dust discharge into chamber. Coal dust velocity magnitude after: a) 4 ms, b) 10 ms, c) 40 ms

Deflagration combustion process because of big speeds is easy to observe as a surface of reaction and a temperature field. Process of coal dust combustion is shown in Figs. 6 (temperature field) and 7 (surface reaction r).

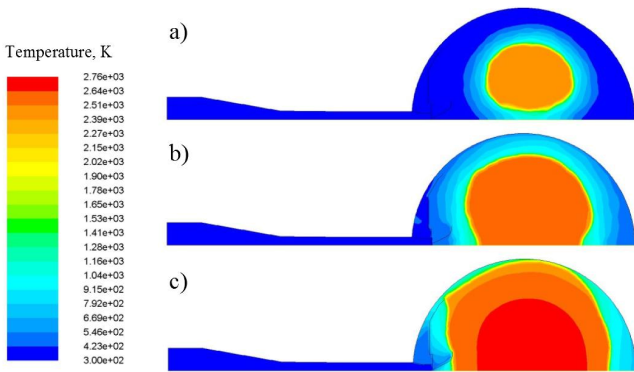


Fig. 6. Temperature field during deflagration combustion of coal dust after: a) 35 ms, b) 40 ms, c) 45 ms

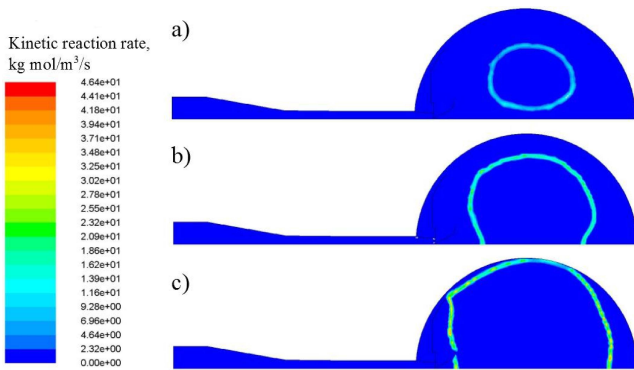


Fig. 7. Reaction of deflagration combustion of coal dust in the test chamber after: a) 35 ms, b) 40 ms, c) 45 ms

The result of numerical simulation is the course of the pressure in spherical tank in the function of time. Dependencies obtained from numerical analysis for coal and flour dust respectively are shown in Figs. 8 and 9.

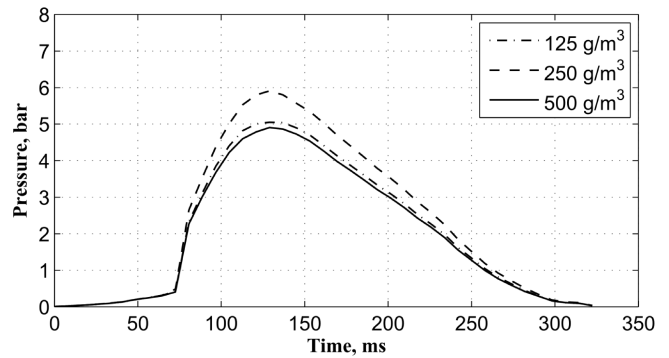


Fig. 8. Pressure changes for the simulation of coal dust explosion

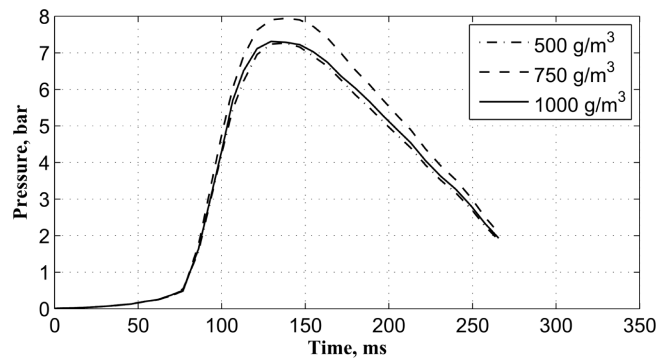


Fig. 9. Pressure changes for the simulation of flour dust explosion

Maximum pressure values of experimental explosions of coal and flour dusts were 7.44 bar (250 g/m^3) and 6.82 bar (750 g/m^3) respectively. Results of numerical simulation do differ slightly from experimental values and amounted to 5.91 bar (250 g/m^3) and 7.95 bar (750 g/m^3) respectively. What is interesting, coal dust achieved maximum pressure of explosion already in 250 g/m^3 , concentration, thus this is why coal dust, taking into account only this parameter, is considered as the most dangerous amongst many dusts used in the industry. Szymanowska flour achieved maximum pressure of explosion only in 750 g/m^3 concentration.

The maximum rate of pressure rise of a dust cloud explosion is pressure increase in time unit coefficient, which determines the speed of propagation of overpressure wave during all explosions of explosive atmosphere in the range of the combustible concentration of dust and in real conditions. Above parameter also influences effects of the dust cloud explosion. The flour dust achieved lower value of maximum pressure increase which amounts to 153.6 bar/s, and coal dust achieved much higher value of 282.99 bar/s. Those values are confirmed by the reports from industry accidents, where effects of coal dust explosions are much more serious than effects of flour explosion. The values of maximum pressure rate rise resulting from the numerical simulations for coal and flour dust were 298.75 bar/s and 231.16 bar/s respectively.

Table 2
Parameters of explosion for coal dust

Dust concentration [g/m ³]	Experiment			CFD		Discrepancy	
	p_{ex} [bar]	p_{max} [bar]	$(dp/dt)_{max}$ [bar/s]	p_{max} [bar]	$(dp/dt)_{max}$ [bar/s]	p_{max} [%]	$(dp/dt)_{max}$ [%]
125	6.87	7.11	243.50	5.05	290.32	29.0	19.2
250	7.15	7.44	282.99	5.91	298.75	20.6	5.6
500	6.74	6.95	273.67	4.91	284.58	29.3	4.0

Table 3
Parameters of explosion for flour dust

Dust concentration [g/m ³]	Experiment			CFD		Discrepancy	
	p_{ex} [bar]	p_{max} [bar]	$(dp/dt)_{max}$ [bar/s]	p_{max} [bar]	$(dp/dt)_{max}$ [bar/s]	p_{max} [%]	$(dp/dt)_{max}$ [%]
500	6.42	6.58	134.22	7.24	196.60	10.0	31.7
750	6.63	6.82	153.60	7.95	231.16	16.6	33.5
1000	6.61	6.80	126.17	7.29	198.53	7.2	36.4

4. Conclusions

Above results of the numerical simulation of process of coal and flour dust deflagration combustion show big opportunities for using of the CFD methods for modelling those processes in course of technological installation designing as well as for emergency situations evaluation. Numerical analysis carried out in FLUENT environment and verified with experimental data, acquired in a laboratory research on the test stand consistent with EN 14034 standard, shows acceptable adaptation of a numerical model to the simulated phenomenon. A discrepancy for researched maximum pressure and a maximum rate of a pressure rise oscillates around 25%, which is a satisfactory result for numerical simulations, which include chemical reactions. Nevertheless, to improve the accuracy of the numerical results the next step planned to be done is a 3D model, a quarter portion of the sphere. It is better to account the 3D effects as well as it is better to address the discharge nozzle geometry. It is assumed that with updated geometry and an improved chemical reaction model, the discrepancies between the experimental and numerical results will be at a satisfactory level. With confidence in numerical results of an explosive combustion process the calculated parameters might be used in a design of the industrial installations for prevention and mitigation of explosion effects.

REFERENCES

- [1] T. Abbasi and S.A. Abbasi, "Dust explosions—Cases, causes, consequences, and control", *J. Hazard. Mater.* 140 (1), 7–44 (2007).
- [2] R.K. Eckhoff, "Understanding dust explosions. The role of powder science and technology", *J. Loss Prevent. Proc.* 22 (1), 105–116 (2009).
- [3] A. Polanczyk, P. Wawrzyniak, and I. Zbicinski, "CFD analysis of dust explosion relief system in the counter-current industrial spray drying tower", *Drying Technol.* 31 (8), 881–890 (2013).
- [4] P. Wawrzyniak, A. Polańczyk, I. Zbicinski, M. Jaskulski, M. Podyma, and J. Rabaeva, "Modeling of dust explosion in the industrial spray dryer", *Drying Technol.* 30 (15), 1720–1729 (2012).
- [5] ASTM E1226, "Standard test method for explosibility of dust clouds", *ASTM Int.* 1, CD-ROM (2010).
- [6] EN 14034, "Determination of explosion characteristics of dust clouds".
- [7] NFPA 68, *Guide for Venting of Deflagrations National Fire Protection Association*, Quincy, MA, New York, 2007.
- [8] VDI 3673, "Pressure release of dust explosions, part 1", *BeuthVerlag GmbH 10772*, CD-ROM (2002).
- [9] W. Barnat, Experimental and numerical study of influence of incidence angle of shock wave created by explosive charge on the steel plate, *Bull. Pol. Ac.: Tech.* 62 (1), 151–163 (2014).
- [10] W. Barnat, Environmental influences on propagation of explosive wave on the dynamic response of plate, *Bull. Pol. Ac.: Tech.* 62 (3), 423–429 (2014).
- [11] B. H. Hjertager, K. Fuhre, and M. Bjørkhaug, "Gas explosion experiments in 1: 33 and 1: 5 scale offshore separator and compressor modules using stoichiometric homogeneous fuel/air clouds", *J. Loss Prevent. Proc.* 1 (4), 197–205 (1988).
- [12] T. Skjold, "Review of the DESC project", *J. Loss Prevent. Proc.* 20 (4), 291–302 (2007).
- [13] U. Krause and T. Kasch, The influence of flow and turbulence on flame propagation through dust-air mixtures, *J. Loss Prevent. Proc.* 13 (3), 291–298 (2000).
- [14] PN-A-74022:2003, "Cereal products. Wheat flour".
- [15] M. Polka, Z. Salamonowicz, M. Wolinski, and B. Kukfisz, "Experimental analysis of minimal ignition temperatures of a dust layer and clouds on a heated surface of selected flammable dusts", *Procedia Eng.* 45, 414–423 (2012).
- [16] Z. Salamonowicz, M. Polka, M. Wolinski, and M. Sobolewski, "Experiments and modeling of ignition of a dust layer on a hot surface", *Przem. Chem.* 93 (1), 99–102 (2014).
- [17] Code ANSYS FLUENT, www.ansys.com.
- [18] K. Jamroziak, M. Bocian, and M. Kulisiewicz, "Energy consumption in mechanical systems using a certain nonlinear degenerate model", *J. Theoret. Appl. Mech.* 51 (4), 827–835 (2013).
- [19] M. Bocian, K. Jamroziak, and M. Kulisiewicz, "An identification of nonlinear dissipative properties of constructional materials at dynamical impact loads conditions", *Meccanica* 49 (8), 1955–1965 (2014).
- [20] G. Sztarbała, "An estimation of conditions inside construction works during a fire with the use of computational fluid dynamics", *Bull. Pol. Ac.: Tech.* 61 (1), 155–160 (2013).